Electrochemical Applications

1/2002

Advances in electrochemical applications of impedance spectroscopy
Issued and © by ZAHNER-elektrik GmbH & Co. KG in June 2002

First of all ...

… we have to say sorry for the long time you had to wait for this new issue of Electrochemical Applications. The delay was mainly caused by two facts: on the one hand we developed a lot of new products like the high current potentiostats of the EL- and the PP-series, the NOISE probe with outstanding features (not only for noise measurements) and the new PC interface which is running under Windows95/98 as well as under WindowsNT/2000 now. On the other hand we had a lot of scientific presentations at well-known meetings which yield enough stuff for the next issues of ***Electrochemical Applications***.

Due to these facts we increased the Zahner team, and I am proud to introduce to you Dr. Werner Strunz, our new co-worker. He studied chemistry in Heidelberg, Germany and took his doctor's degree on "Electrical Conducting Coordination Polymers". He is supporting the Zahner team in several software projects and – above all – he is enhancing our scientific work. You will find him as a co-author of various scientific presentations.

The recent issue of ***Electrochemical Applications*** does focus not only on EIS but on associated methods which are able to complement EIS in specific applications. First of all, there is the HCI (***H***igh ***C***urrent ***I***nterrupt) method, which allows you to find results in low impedance objects such as power generating devices even at high frequencies. The relaxation voltammetry is an alternative method for investigating high impedance systems such as coatings. The EIS chapter of this issue comes from Dr. Hoffmann (MTU-Friedrichshafen GmbH) who is demonstrating the application of *AC impedance spectroscopy on molten carbonate fuel cells*.

We hope, the topics of this issue are a good excuse for the long waiting period.

Your Zahner Team

Current Interrupt Technique - Measuring low impedances at high frequencies

F. Richter, Siemens AG, KWU, Erlangen, Germany, franz.richter@erl11.siemens.de
C.-A. Schiller, Zahner-elektrik, Kronach, Germany, cas@zahner.de
N. Wagner, DLR, Stuttgart, Germany, norbert.wagner@dlr.de

If a power generating device is examined, its dynamic electrical equivalence generally will appear as a network which represents anode, cathode, membrane, electrolyte, and connectors.

The specific losses of every partial impedance of the network contribute to the overall efficiency of the device. The porous layers of anode and cathode, responsible for the charge transfer reaction, normally play a major role. Other contributions seem to be much less important. There is the resistance of the electrolyte or the membrane as well as the resistance of contacts and connectors. A dynamic part is added by the inductance of the body and the connectors.

Nevertheless, the ohmic part (electrolyte, membrane, connectors) plays an important role regarding the performance of the device and accounts sometimes for the main part of the overall losses. It is very sensitive to degradation caused by corrosion and thermal stress.

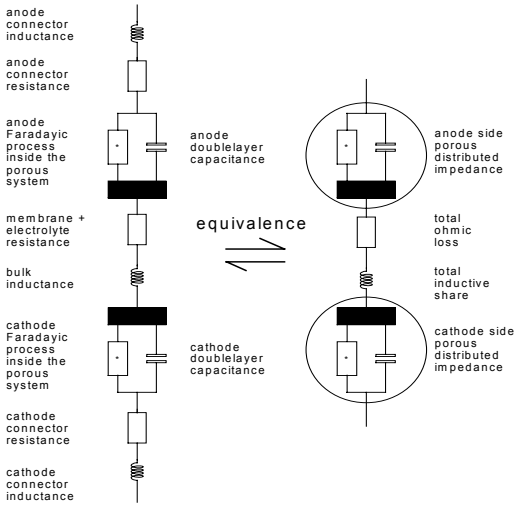

Fig. 1: Simplified electrical equivalent circuit of a typical electrochemical power source device

In applications with dynamic load changes the inductive parts, for example in a laptop computer battery or in electromotive applications, are limiting the maximum pulse load available.

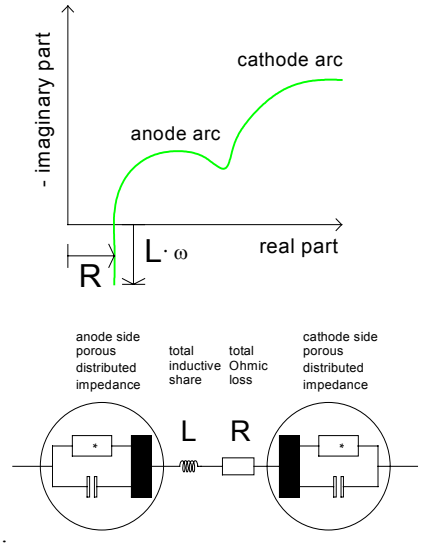

Fig. 2: The appearance of ohmic share and stray inductance in a fuel cell spectrum

EIS allows to separate all contributions and to determine the ohmic part in the high frequency region of a spectrum, where the impedance curve intersects the real axis. The inductance is shown at successive higher frequencies in the diagram. But there is one great restriction: Measuring impedance always means to measure two signals, current and voltage.

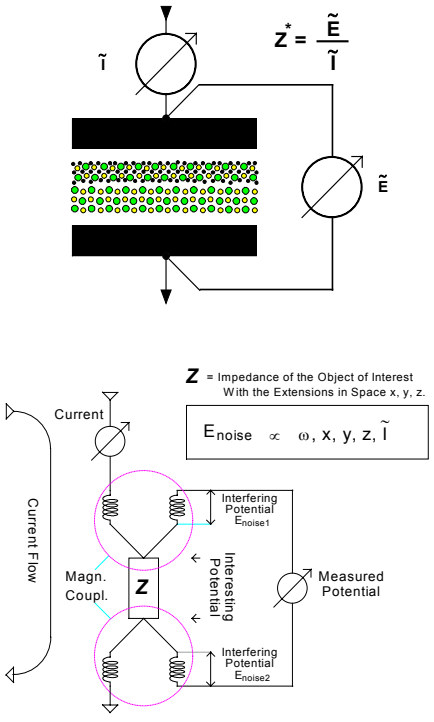

Fig. 3: Basic impedance measurement circuit – principle (top) and detail (bottom)

A closer look at the circuit in figure 3 shows that the potential information does not only contain the interesting part from the site of the connecting terminals. It is rather contaminated by dynamically induced error voltages. These errors are caused by unavoidable mutual induction from the magnetic field of the current circuit.

The interference increases with increasing frequency and with the strength of the magnetic field of the current. It depends on the geometry and grows with the dimensions of the object. For the investigation of power sources this means: The more you scale up, the lower is the available upper frequency limit (f_g). Finally, there is a limit for the EIS at low ohmic objects. At a rough estimation you can calculate with:

$$f_g \approx 1\ \text{MHz} * |Z|_{min} / \text{Ohm}$$

As a consequence, the window for getting an Ohmic resistance information by means of the EIS gets smaller for bigger cells. For certain systems, the window will be closed.

What can be done to complement the EIS under these conditions? The question is answered by the well known current interrupt technique, which does not need the knowledge of two signals simultaneously. The principle is depicted in figure 4 and explained in the following:

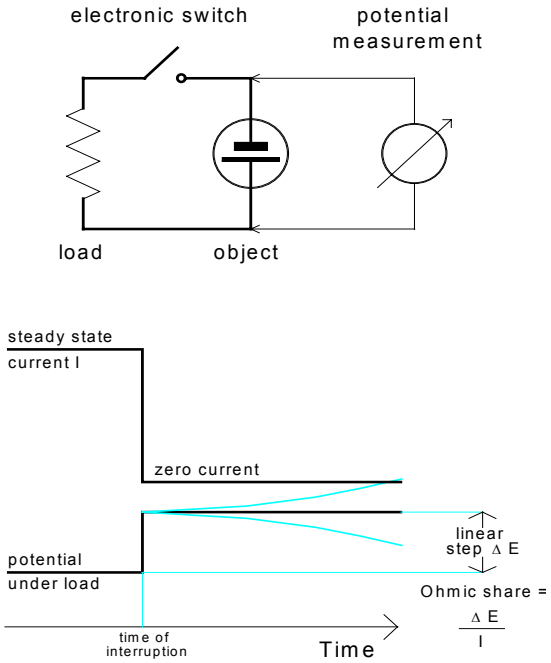

Fig. 4: Principle of current interrupt technique to determine the ohmic share

A steady-state current is interrupted by a switch. The step response of the potential is sampled and analysed assuming that the current drops instantaneously from its stationary value to zero.

In practice, the settling time depends on the electromagnetic energy stored in the parasitic capacity

and inductivity of the cell arrangement on the one hand and the damping process on the other hand. Provided that the set-up is built appropriate, the interruption results in a breakdown of the current to at least small values within a short time. In this case, the potential will be disturbed much less by mutual induction compared with an EIS measurement.

In theory, the ohmic contribution to the overall impedance can be easily seen from the height of the fast rectangular step of the potential. For the evaluation a linear step model is commonly used.

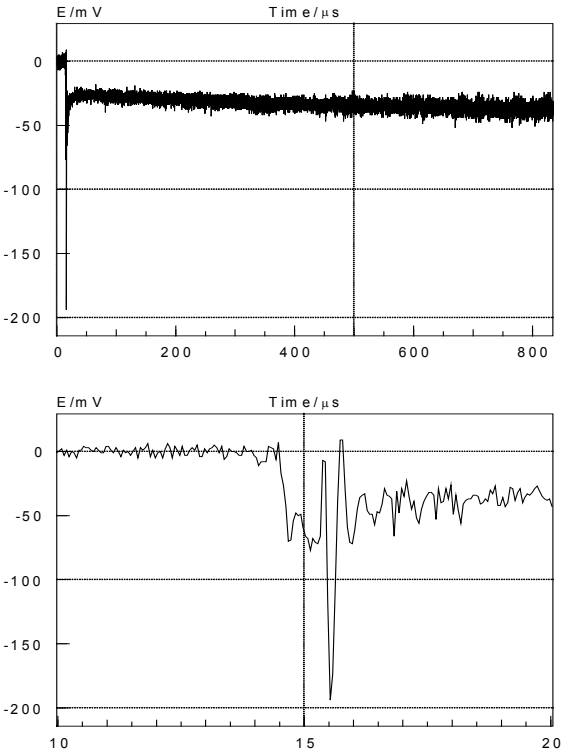

Fig. 5: Typical current interrupt potential step response. Long (top) and short (bottom) term response of a single cell PEM fuel cell at 80 A.

But this evaluation suffers from the fact that the analysis of the time domain data is interfered by the "ringing" in the signal as a result of the parasitic resonance. In addition, the early phase of the response is characterized by a non-linear behavior due to the imperfect characteristics of the electronic switch. Furthermore, the response of both double-layers may follow soon after the interruption when the concentrations of the involved species turn from their steady state values to new ones without load. All these effects bend and distort the expected ideal shape of the potential step. Therefore, the automatic analysis of pulse measurements by means of a simple fit to a linear step model often leads to inaccurate results.

Our aim was to improve the method in order to get results of comparable reliability to the EIS. The basic idea is not to evaluate the distorted step function in the time domain. Instead, after a transformation of the data into the frequency domain, the resulting spectrum and all parasitic effects can be analysed by means of EIS methods.

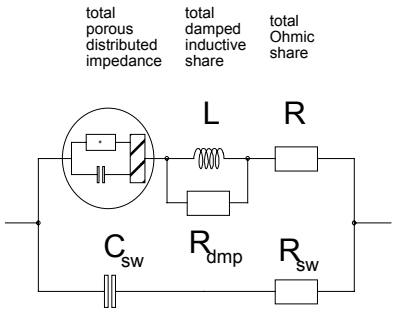

C_{sw},R_{sw}: Capacitance and resistance of the electronic switch.
R_{dmp}: Damping of the inductive share due to spatial distribution.

Fig. 6: Approximate equivalent circuit for a complete high current interrupt measurement set-up of an electrochemical power source device.

In figure 6, a simplified equivalent circuit for a complete HCI measurement set-up of a power cell is shown. It contains the impedance of the active cell part (circle), the integral inductance (L) and resistance (R) and the parasitic effects of the switch circuit. The resonance circuit is mainly built of the series inductance, the double layer capacity and the capacity of the electronic switch. It is responsible for the overshot and "ringing" in the pulse response signal.

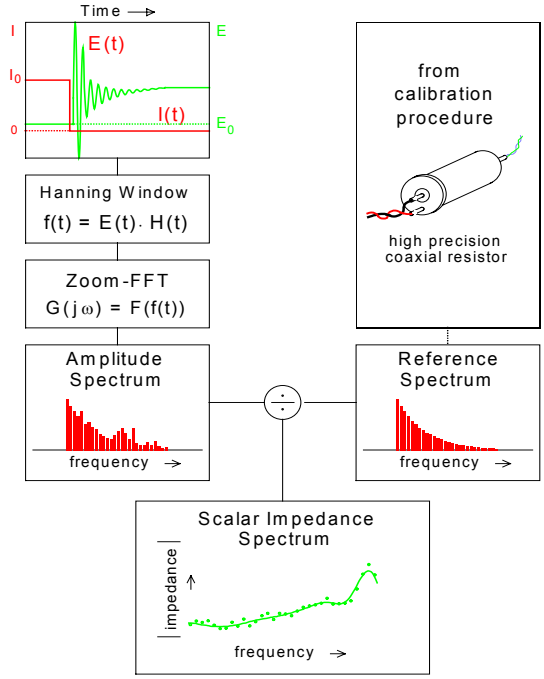

Fig. 7: Principle scheme of the Zahner high current interrupt data processing.

Figure 7 illustrates the essential steps for the transformation of the time domain data into the frequency domain. The potential response signal E is sampled by a transient recorder. The numeric algorithms use discrete Fourier transform methods to achieve an effective analysis. In order to minimize the errors caused by their application on single events, a

weighing function has to be applied. At least, a *Zoom FFT* calculates the amplitude spectrum in the frequency domain. A similar procedure using a reference resistor was done for calibration. The quotient of both spectra finally leads to the modulus of the impedance of the unknown object.

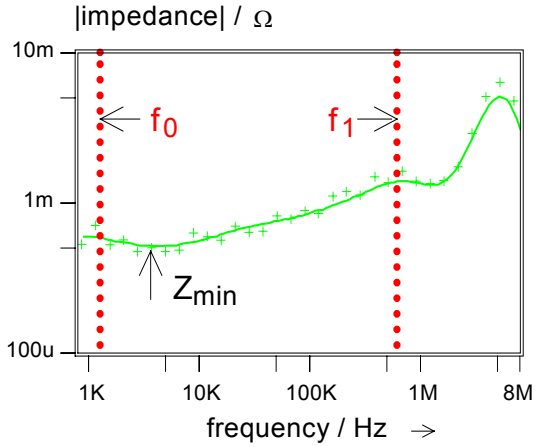

Fig. 8: Automatic evaluation of the ohmic share from the scalar impedance function.

This scalar impedance spectrum can be used to evaluate the ohmic share in a simple, automated way: The user selects a reliable frequency range for analysis, which excludes the parasitic resonance at the high frequency end. The impedance minimum within this range represents the ohmic share with an acceptable accuracy of about 1 to 3%.

If you want to evaluate the response spectrum with the standard methods of the EIS, beside the impedance, the phase data will be necessary: For this calculation a relation between impedance and phase for all two pole impedance objects of minimum phase can be used. The ZHIT[1] relation allows to calculate the modulus of the impedance course from the course of the phase angle. It will also be able to perform the inverse application, if one uses the ZHIT in an iterative numeric way. This is the way, our analysis software obtains a complete spectrum.

The complex spectrum can now be analyzed in the usual way, for instance, by means of simulation and fitting of the equivalent circuit. According to our experience, the ohmic share can be determined in this way, with typically the double or triple accuracy compared to the automatic minimum detection in the scalar impedance function.

Figure 10 is a sketch of the practical set-up of our high current interrupt measurement arrangement of a fuel cell. The electrochemical cell (A) is supplied by means of an electronic load (B) or another type of high power potentiostat to force the steady state load conditions. Additionally, the potentiostat acts as fast electronic switch for the current interruption.

[1] W. Ehm, R. Kaus, C.-A. Schiller, W. Strunz: ZHIT - a simple relation between impedance modulus and phase angle... Electrochemical Society Proceedings 2000-24, 1

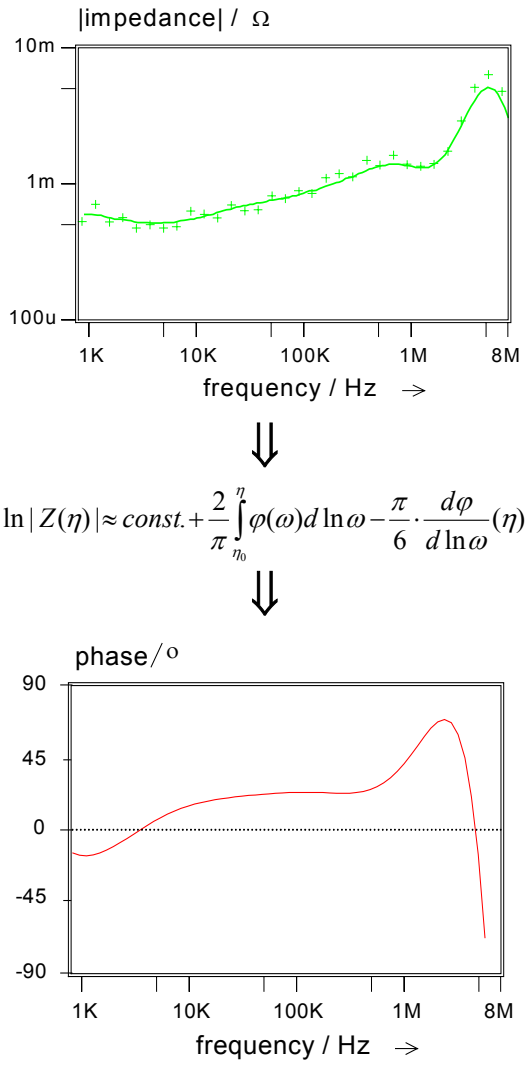

Fig. 9: Calculation of the phase angle from the impedance modulus by means of the inverse application of the ZHIT[1] transform. The ZHIT equation shows that the impedance modulus at the frequency η can be calculated from the integral of the phase angle course φ(ω) within limited frequency boundaries (η_0 to η). A correction term proportional to *dφ/d*lnω enhances the accuracy.

The potentiostat is controlled by an electrochemical workstation (D) including a high resolution transient recorder. The recorder input is connected to the potential sense lines of the cell along a so called pulse probe (C). The main task of the pulse probe is the galvanic isolation of the potential sense circuit from the instrument in order to minimize electromagnetic interference. On the other hand, it is responsible for the protection of the instrument input by means of an energy consuming clipping circuit.

After a short 'sampling shot' during the interrupt, the instrument switches on the current again, in order to re-establish the steady state and to avoid potential damage of the cell. The pulse response is analyzed then by the software of the workstation as described before.

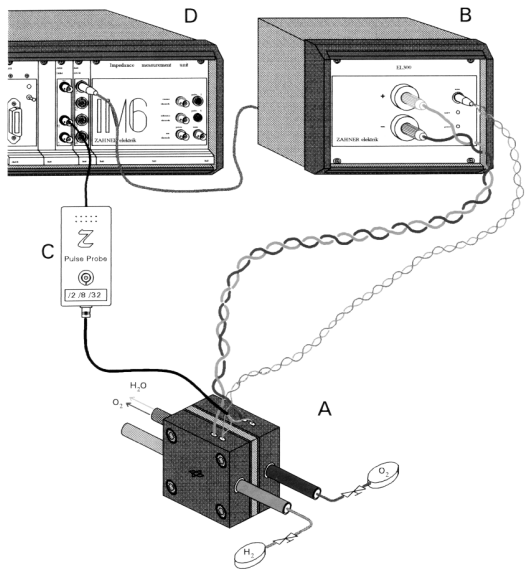

Fig. 10: Practical set-up of a high current interrupt fuel cell measurement arrangement

A lot of test experiments under controlled conditions have been done. The major experience is that, compared with the standard EIS, the HCI is much less sensitive to mutual induction artefacts. This is illustrated by the example depicted in figure 11. Here, we made test measurements at resistors using two different, intentionally non-optimized connection geometries. As you can see, the strong in-phase mutual induction of the above example leads to an inductive component which seems unrealistically high in the case of the standard EIS. The HCI method, however, leads to the almost exact value.

With the other example, which shows a strong out-of-phase mutual induction, one obtains almost the same impedance functions, which has been omitted here. Yet, the phase diagram shows paradox behaviour for the standard EIS curve: The course indicates capacitive characteristics! The phase curve of the HCI experiment shows the correct sign due to its origin from the ZHIT transform.

We also found that the HCI worked fine with power generating devices. As an example, the results of an EIS and a HCI experiment at a high temperature fuel cell are depicted in figure 12. The cell has been driven with air and humidified hydrogen and generated more than four Amperes at a potential exceeding 0.73 Volts. In both experiments the best case wiring was used to reduce the mutual induction contribution.

The original HCI potential step response is plotted on top of figure 12. At the bottom, the transformed impedance (circles) as well as a comparative impedance measurement (rhombi) are drawn. As one can see, the methods complement each other for the different frequency ranges. In this special case, the frequency limit for the EIS experiment to get accurate information on the ohmic share is not exceeded. Therefore, both methods deliver the correct results.

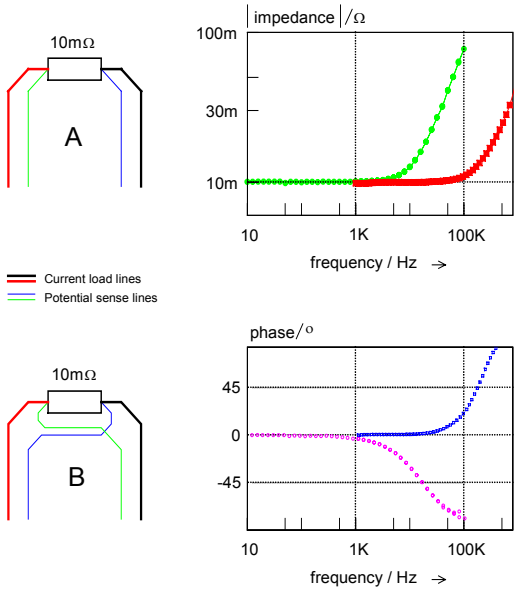

Fig. 11: Results of test measurements at reference resistors incl. mutual induction (MI) components.
A: In phase MI leads to a high inductive response in the case of EIS (full dots) whereas the HCI spectrum (squares) matches the theory.
B: Out-of-phase MI causes paradox capacitive (-) EIS phase courses (squares) while the HCI phase course shows the correct phase sign for inductance (+).

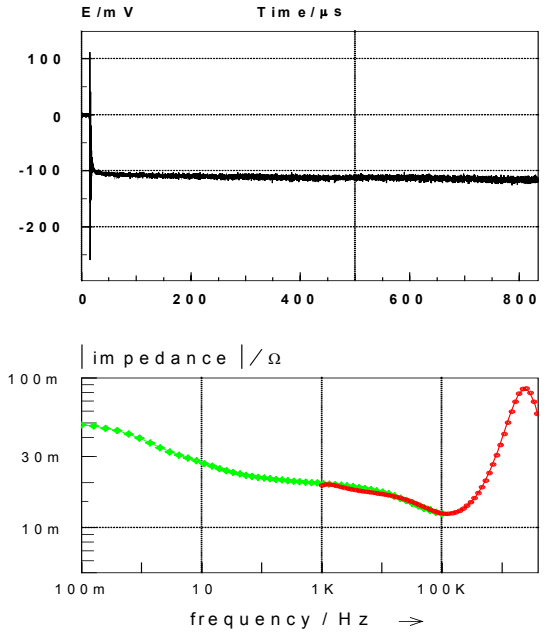

Fig. 12: High current interrupt measurement of a single solid oxide fuel cell at 866°C.
EIS: 100 mHz – 100 kHz (rhombi)
HIC: 1 kHz – 800 kHz (circles)

The last example demonstrates that the dominating error from the unavoidable mutual induction falsifies the result of standard EIS measurements at very low impedance objects. In the experiments depicted in figure 13, a HCI measurement (top) as well as a comparative EIS measurement (bottom, triangles)

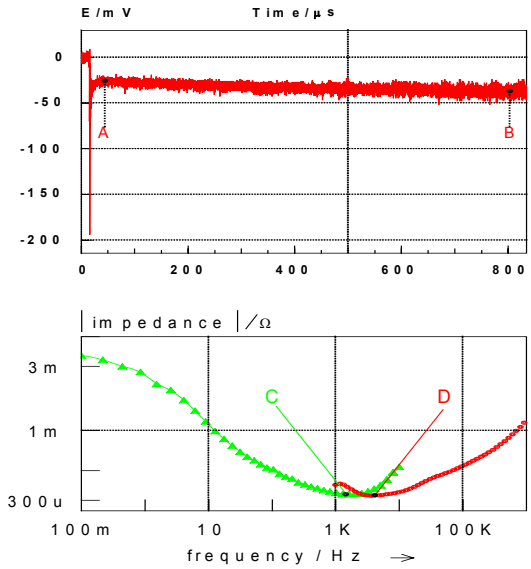

Fig. 13: High current interrupt measurement of a single PEM fuel cell at 85° C and 80 A. The resulting spectrum (C) is compared with a standard EIS (D).

on a big PEM fuel cell at a current of 80 A were performed. The shift of the increase of the impedance for the transformed HCI-data (circles) to higher frequencies indicates the smaller sensitivity of the HCI measurement against the mutual induction.

In our opinion, the missing correspondence between the EIS- and the HCI-data at the low frequency end of 1.1 KHz results from a non-linear component in the long term pulse response signal. HCI analysis has to rely on the rule of linearity. The transient changes of about -10 mV within the 0.85-milliseconds-analysis-interval may be enough to violate this rule.

Conclusion

1. EIS capabilities are basically limited by mutual induction at the high-frequency low-impedance edge. This falsifies significantly the results for ohmic and inductive share.
2. The HCI capability is limited by the magnetic energy stored in the load circuit.
3. The HCI analysis can be automatically analyzed reliably by transforming the time data into the frequency domain.
4. According to our experience, HCI can extend the available frequency range about a factor of three to ten in a carefully optimized experimental set-up.
5. HCI data interpretation should not be extended to the low frequency response. The unavoidable violation of the EIS linearity rule after a certain interruption time may lead to misinterpretations.
6. Thus, an arrangement which performs both, the standard EIS and the HCI measurement within one set-up, is the best choice for the challenges of electrochemical power source device testing.

Relaxation Voltammetry
A technology for the evaluation of barrier coatings

Werner Strunz, Zahner-elektrik, Kronach, Germany, wos@zahner.de

Introduction

Products made of steel have excellent mechanical properties. In addition, steel is an inexpensive material and therefore, iron in the form of steel is one of the most important technical raw materials of the daily life. Unfortunately, the chemical characteristics of steel are not so favourable. As a base metal, iron is sensitive to oxygen and humidity. As a consequence, unprotected steel corrodes very easily and the corrosion process not only affects the optical appearance but also influences the mechanical properties unfavourably.

One way to protect iron against corrosion is the application of organic coatings. The development of new coatings requires methods to optimise the formulation which have to be tested during their development by the coatings manufacturers. To obtain a ranking of the corrosion protective performance of new coating formulations, many different weathering tests are necessary. After the weathering, the degradation of the coating has to be evaluated using mainly mechanical tests or visual examination. These tests are time consuming and the degree of degradation has to be estimated. The need of an objective and relatively fast evaluation method is obvious. Here, electrochemical impedance spectroscopy (EIS) is widely used for the characterization as well as for the detection of defects of the coating. Moreover, this method is also applied for the determination of the water uptake and the degree of blistering and delamination. EIS provides information about the mechanistic background of corrosion processes as well as detailed information about coating properties like capacity C_C or coating/pore resistance R_C.

For the interpretation of EIS-data, physical models like equivalent circuits are required. The basic models are given in figure 1. Model A describes a realistic perfect 'barrier coating' with the coating capacity C_C and the coating/pore resistance R_C. Model B represents the case of pores and defects in the coating with a second 'time-constant', which is correlated to the charge transfer, i. e. the charge transfer resistance R_{CT} and the double layer capacity C_{DL}. This model is widely used in many publications of EIS-results.

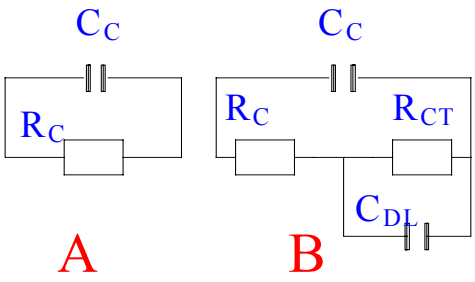

Fig. 1: Most popular basic equivalent circuits for the interpretation of EIS data

Unfortunately, the application of EIS in corrosion research shows some handicaps. For instance, commercially available 'barrier coatings' often show a low-frequency resistance around 10^{10} $\Omega \cdot cm^{-2}$ or more. This requires a 'low frequency limit' of the measured spectrum in the mHz-region for the determination of R_C. Such measurements are rather time-consuming. They can easily exceed one hour.

Next, the measured system has to be in a steady state during the whole measuring time. Concerning water-uptake measurements for instance, it is save to assume that the constancy of the coating parameters (i. e. C_C and R_C) is not given in the early state of immersion. At least, considering the ratio of the number of measured specimens and the time required for a single measurement, a single impedance measurement seems to be rather expensive.

In contrast to measurements of barrier coatings in the frequency domain, traditional methods in the time domain suffer from the special properties of this kind of systems. For instance, static DC-measurements enable the determination of R_C, but will not deliver any information of dynamic parameters, neither about the dielectric properties nor about 'dynamic' processes (like diffusion contributions) within the coating. Dynamic measurements in the time domain which are reported in the literature [1,2], i. e. current interrupt techniques, suffer from the high resistances of the coating materials too. On one hand, so-called electrometers have an excellent accuracy in measuring current. Unfortunately these electronic devices possess a poor resolution in time[2]. Due to this fact, these instruments are not able to monitor (or to separate) fast processes. On the other side, the current interrupt technique reported in the literature [2], delivers a resolution in measuring current of only 120 pA/digit. As will be shown below, this resolution is by far too small.
A relatively new technology for the investigation of high-ohmic systems is the *Relaxation Voltammetry* (RV) [3-6]. This method is a current interrupt technique too, but was designed especially to overcome the problems noted above. The principle of this technique is depicted schematically in figure 2 and explained in the following.

[2] Usually, small currents are measured by integration a voltage drop at a shunt-resistor. But, the smaller the current the longer the time of integration for a given accuracy. As a consequence, the sampling rate of an electrometer is less than one point per second at the pA–level [1].

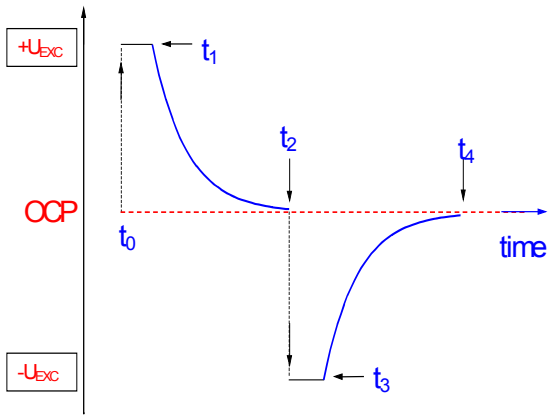

Fig. 2: The principle of RV

The potential $+U_{EXC}$ is superimposed to the open circuit potential (OCP) and causes a transient current (I_{EXC}) which tends to be constant after a certain time (t_1-t_0 = t_{EXC}). After the current reaches this stationary state, it is switched off and the following decay of the potential U(t) is recorded as a function of time (t_1 to t_2). The initial stage of this relaxation process is monitored using a sampling rate of 600 points per second (about 40 to 100 values) and then the sampling rate is lowered. After the potential reaches approximately the value of the OCP (at t_2 in figure 2), the procedure is repeated using the same potential but with the opposite sign ($-U_{EXC}$).

Concerning the following considerations, the experimental procedure of RV differs essentially from 'traditional interrupt techniques':
1. In general, each electrochemical experiment is characterized by two parameters, potential and current. In potentiostatic mode of operation for instance, a potential is applied whereas the corresponding quantity (the current) is measured as a function of the actual potential. In contrast, in RV, a constant potential is applied and after interrupting the current, again the potential is recorded as a function of the relaxation time. This kind of operation offers mainly two advantages. First of all, a potential in the range of 10^{-3} to 10^{-6} V can be measured more precisely than a current in the range of 10^{-12} to 10^{-15} A in principle. Secondly, the current (±) I_{EXC} is measured at its highest level, integrating over a small interval (about five seconds) before the interrupt which improves the accuracy additionally.
2. Anodic **and** cathodic excitation are performed and both transients are measured. For the evaluation of the transient response U(t), the values of both half-cycles are averaged, resulting in a 'symmetrical square-wave perturbation' around the OCP - similar to EIS.
3. This 'symmetrical' operation is important, considering the experimental fact obtained from measurements of barrier coatings that the transients will not return exactly to the value of the OCP before the excitation. In a continuous mode of operation, t_{EXC} and/or U_{EXC} can be varied in subsequent cycles. Performing only anodic **or** cathodic excitation - like

in 'traditional interrupt techniques' - would result in a shift[3] of the OCP. This would lead to erroneous results due to a superimposed (rest-) relaxation caused by the offset between the 'end-potential' (at t_2/t_4 in figure 2) and the OCP. To overcome this problem, in RV the OCP is 'updated' after each half-cycle from the values of the 'end-potential' of the actual and the latter half-cycle (for instance: OCP = ½ (U_{t4} + U_{t2}).

The applicability and performance of RV can be best represented by an example and in comparison to a measurement using EIS. In figure 3, the result of an RV measurement of a barrier coating is plotted as a function of the square root of 'the relaxation time (upper diagram) whereas an impedance spectrum of the same specimen is shown at the bottom of figure 3.

The DC accuracy of RV is best reflected regarding the small value of I_{EXC} (1.33 ± 0.01 ·10^{-12} A), resulting from the total DC-resistance of the coating (1.5·10^{10} Ω or 6.75·10^{10} Ω · cm^{-2}) [4]. The small diagram on the right side of the upper part of figure 3 shows the initial voltage decay of the relaxation as a function of time. As indicated in the figure, the early state of the relaxation was measured with the higher sampling rate. The evaluation of this part of a RV-transient delivers information about the dielectric properties of the system under investigation and therefore gives an estimate of the dynamical performance of RV. This part will be discussed below in detail.

Comparing the results of EIS and RV in figure 3, the complementary nature of both techniques becomes aware. Considering the time (frequency) scale of both methods, one has to conclude that EIS handles the high frequency part (say above 1 Hz) accurately and without consuming too much time for the measurement. But at lower frequencies, the measuring time increases drastically which restricts the number of measured points (i. e. only 5 points below 1 Hz in the above example) in practical measurements in a coating manufacturer's laboratory which may result either in a loss of accuracy or of information.

On the other side, RV handles the middle and large relaxation range (above 1 second) which corresponds to the 'middle and low- frequency part' of an impedance spectrum very well. This fact is simply expressed by the number of measured points (n > 2500 above 1 second). A sufficient 'overlap' between the time scale of both methods arises from the initial sampling rate of RV which is shown in the following.

The 'dynamic' performance of RV

As noted above, the total DC-resistance R_T can be calculated immediately from the applied potential (±U_{EXC}) and the current (±I_{EXC}) before the interruption. In addition, RV delivers the coating capacity C_C without the need of a detailed interpretation of the

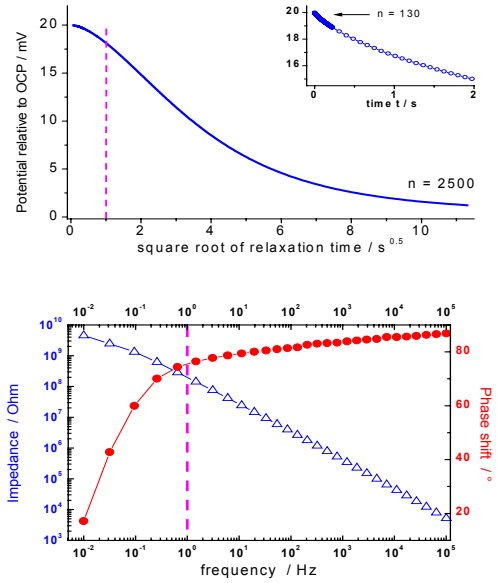

Fig. 3 : RV and EIS as complementary techniques (see text)

overall relaxation process. Adopting the models for the interpretation of EIS-data (figure 1), this parameter is accessible from the initial slope (ISL) of the potential decay and I_{EXC} (scheme 1). From a theoretical point of view, the determination of C_C founded on the ISL is exact for model A and an excellent approximation in the case of model B[5]. If necessary, the applicability of the ISL approach can be extended mathematically, involving the quadratic term of the underlying power series (ISL_{EXC}).

$$U(t) = I_{EXC} R_T \cdot e^{-\frac{t}{R_T C_C}} = I_{EXC} R_T - \frac{I_{EXC}}{C_C} t + \frac{I_{EXC}}{2 \cdot R_T \cdot C_C^2} t^2 \pm \ldots$$

$$ISL = \lim_{t \to 0} \frac{dU}{dt} = -\frac{I_{EXC}}{C_C}$$

$$ISL_{EX} = \lim_{t \to 0} \frac{dU}{dt} = -\frac{I_{EXC}}{C_C} + \frac{I_{EXC}}{2 \cdot C_C^2 \cdot R_T}$$

Scheme 1 : The initial slope approximation (ISL)

From a practical point of view, the scope and accuracy of the ISL approximation was first verified by measurements at the equivalent circuits. From the results of these measurements [3-6] the accuracy of the determination of C_C is about 10% or less for typical values which are observed when measuring coating materials, i. e. capacities in the range of ≥100 pF and total DC-resistances of ≥50 MΩ respectively. Two examples for the determination of C_C' using the ISL approximation are depicted in figure 4.

[3] A similar effect which is commonly observed in water-uptake measurements results from the drift of the OCP caused by the measured system itself.
[4] Measuring area : 4.5 cm^2

[5] The physical background of this approximation is that the current through the capacitor C_{DL} can be neglected at the initial stage of the relaxation and therefore, model B in figure 1 reduces to model A.

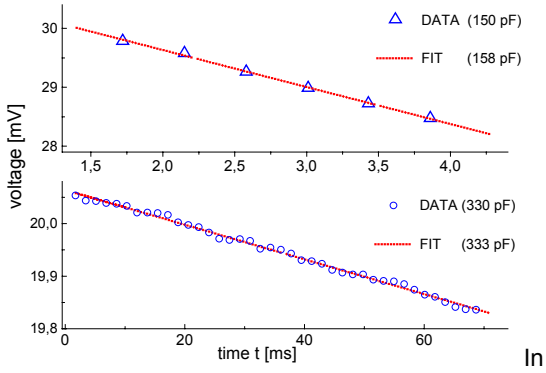

In

Fig. 4 : ISL of two dummy cells (model B)

In the upper part of the diagram an equivalent circuit (model B) with a total resistance R_T of 305 MΩ and a 'coating capacity' of 150 pF is shown. From the voltage decay (≈ 2mV) in the first 4 milliseconds, an initial slope of -630 mV/s can be evaluated. Considering the current I_{EXC} (98.4 pA) yields a coating capacity of 158 pF. In the second example an equivalent circuit (model B) with a total resistance R_T of 18.7 GΩ and a coating capacity of 330 pF was used. The potential decay (≈ 200 μV) in the first 60 milliseconds gives an initial slope of -3.3 mV/s. With the current I_{EXC} (1.1 pA) a coating capacity of 333 pF was calculated. The latter example demonstrates additionally that noise effects play no role at all at this early state of the relaxation. In both cases an excellent agreement between theoretical and experimental data results.

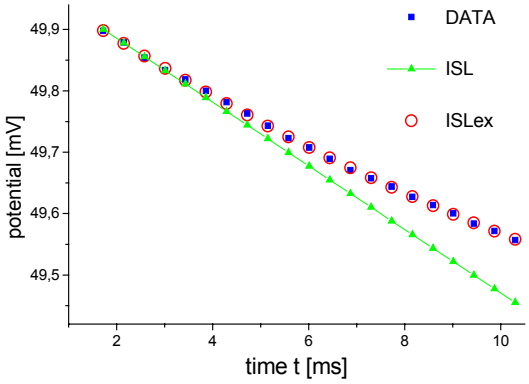

Fig. 5 : Typical ISL of a coating

Figure 5 shows a typical example for the evaluation of C_c of coatings using the ISL method. The voltage drop (squares) in the first 10 milliseconds is about 500 μV. Comparing the starting potential decay with the values obtained from dummy measurements it becomes evident that the linear range turns out to be much shorter than predicted from the models given in figure 1. The deviation from linearity (triangles = ISL) occurs already below 4 milliseconds. To evaluate the coating capacity the extended ISL_{EX} (circles) was used, therefore. The analysis of the linear part gives an initial potential decay of -53 mV/s, yielding a coating capacity of 250 pF.

Further applications of RV in corrosion research of coated metals are reported in more detail in the literature [4, 7-9].

In a comprehensive analysis of a huge number of different coating materials over a wide range of relaxation times it was found that the dielectric relaxation in barrier coatings can be explained by a hopping (i. e. a random walk) process [10]. It is noteworthy that this so-called 'two-step continuous time random walk' (CTRW-2) exhibits a square root of time dependency of the corresponding time-law which seemed to contradict the results of EIS (see also [11,12]). However, in two recent publications [13,14] it was proven that there is no contradiction at all between the interpretation of the results of both techniques in principle, concerning the evaluated dielectric parameters.

Summary

It was shown that RV is a suitable tool for the investigation of high ohmic systems. Although other applications can be seen, RV was especially designed to meet the demands for the investigation of coated metals.

In contrast to 'traditional interrupt techniques', RV combines electrometer-type accuracy with an adequate resolution in time so that DC- as well as dielectric parameters of these systems are accessible. Both quantities are of great importance for the coatings manufacturer to improve their products. In comparison to EIS it is to state that both techniques should supplement each other ideally. Undoubtedly, the big advantage of EIS for the evaluation of high ohmic systems is the rapid determination of the dielectric properties whereas the strong points of RV are in the 'middle and low frequency range'. At least, the RV equipment is less expensive so that several measurements can be performed in parallel which reduces the time consumption in the manufacturer's laboratory additionally.

References

[1] Granata, R. D.; Kovaleski, K. J., 'Evaluation of High-Performance Protective Coatings by Electrochemical Impedance and Chronoamperometry' in 'Electrochemical Impedance : Analysis and Interpretation'; eds. : Scully, J. R.; Silverman, D. C.; Kendig, M. W.; ASTM STP 1188 (1993)

[2] Tanabe, H.; Nagai, M.; Matsuno, H.; Kano; M.; 'Evaluation of protective coatings by a current interrupter technique' in 'Advances in Corrosion Protection by Organic Coatings II' (1994); ISBN 1-56677-108-0; pages 181 – 192; (from : *Materials and Corrosion* **47** (1996), abstract nr. 96-0831)

[3] G. Meyer, H. Ochs, W. Strunz, J. Vogelsang; 'Barrier coatings with high ohmic resistance - comparison between Relaxation Voltammetry and Impedance Spectroscopy'; Proceed. of EMCR 1997, 25. - 29. -8. 1997, Trento Italy, oral contribution

[4] G. Meyer, H. Ochs, W. Strunz, J. Vogelsang; *Materials Science Forum,* **289-292** (1998) 305

[5] H. Ochs, W. Strunz, J. Vogelsang; 'Relaxation voltammetry with organic barrier coatings on steel - experimental and theoretical approach'; Proceed. of EMCR 1997, Trento, Italy, poster presentation

[6] G. Meyer, H. Ochs, W. Strunz, J. Vogelsang; *Materials Science Forum,* **289-292** (1998) 373

[7] W. Strunz, J. Vogelsang; 'Characterization and evaluation of organic coatings using relaxation voltammetry'; Proceed. of EUROCORR 1998, Utrecht, Netherlands, oral contribution
[8] J. Vogelsang, W. Strunz; 'Barrier coatings - a challenge for EIS and RV'; Proceed. of EIS 1998, Rio de Janeiro (Brasil).
[9] J. Vogelsang, U. Eschmann; G. Meyer, W. Strunz; 'Eisenglimmer in Korrosionsschutzbeschichtungen – neue Erkenntnisse zum Wirkmechanismus'; *Farbe & Lack* **104**:5 (1998) 28.
[10] W. Strunz; 'Dielectric Relaxation in Barrier coatings – a square root of time process'; *Prog. Org. Coat.* **39** (2000) 49
[11] J. Vogelsang, W. Strunz; 'Electrochemical investigations of organic, corrosion protective barrier coatings - limiting factors of small signal perturbation techniques'; *Materials and Corrosion* **52**:6 (2000) 462.
[12] J. Vogelsang, W. Strunz; 'New interpretation of electrochemical data obtained from organic barrier coatings'; Proceed. of 7th Int. Symposium on Electrochemical Methods in Corrosion Research, Budapest, Hungary, (2000); Electrochimica Acta, **46** (2001) 3817
[13] C. A. Schiller, W. Strunz; 'The evaluation of experimental dielectric data of barrier coatings by means of different models'; Proceed. of EMCR 2000, Budapest, Hungary; oral contributions at EMCR 2000, Budapest, Hungary (2000) and ISE 2000, Warsaw, Poland (2000); Electrochimica Acta, **46** (2001) 3619
[14] W. Strunz; '*The frequency behavior of the 'two-step' continuous time random walk*'; Proceed. of EMCR 2000, Budapest, Hungary, oral contribution (2000)

AC-Impedance Spectroscopy on Molten Carbonate Fuel Cells

Joachim Hoffmann, MTU-Friedrichshafen, Munich, Germany, HoffmannJ@mtu-friedrichshafen.com

Introduction

AC-Impedance Spectroscopy has a broad range of application in electro-analytical chemistry. During the last years increasing efforts have been made to analyze the processes contributing to the reactions, happening inside fuel cells. Here the AC-impedance spectroscopy yields a variety of useful information.

MTU-Friedrichshafen GmbH is involved in the research and development of *Molten Carbonate Fuel Cells* (MCFC) since 1993 and began to use Zahner instruments (IM5d) in 1995. Later several IM6 systems and electronic load banks EL100 and EL300 completed the actual instrumentation. The measurements were rather useful to identify the effects of several modifications on the electrochemical active components of the MCFC. Some of the observations will be described in the next chapters.

Experimental

A MCFC of the MTU-type consists of a Ni-Anode, a $LiAlO_2$-Matrix and a NiO-cathode. The lithiation of the cathode proceeds during the first 100 h of operation at 650°C. The operating gases are $H_2/CO_2/H_2O$ = 73/18/9 Vol% with H_2-utilization of 75% at 160 mA/cm2 on the anode side and $O_2/CO_2/N_2/H_2O$ = 9/13/73/5 Vol% with O_2-utilization of 33% and CO_2-utilization of 50% at 160 mA/cm^2 on the cathode side. Most of the cells were operated under constant flow conditions.

Results and Discussion

First of all it must be remarked that the electrodes of fuel cells have an extremely high porosity. This porosity has a severe impact on the results of the AC-impedance spectroscopy. Displaying the impedance data in a Nyquist-diagram normally one would expect semicircles. For porous electrodes these semicircles are somewhat compressed and appear more or less as circle-segments.

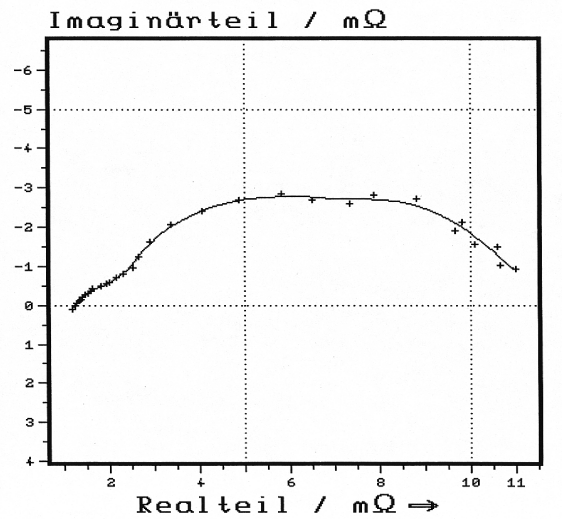

Fig.1: Cell impedance as a Nyquist plot.

This shape makes it rather difficult to generate a calculated curve by Zahner's fitting technique, since an element has to be defined, which should contain the properties of the porous body. This becomes even more difficult since the circle-segment may contain a number of independent circle-segments and displays the "sum" impedance of all relevant processes.

At this point the fitting of the curves comes close to fortune telling. Here it is impossible to get any reliable quantitative information from the system.

On the other hand it can be more helpful to display the impedance data in a Bode-diagram. Here the information is split into the recorded impedance and the phase-angle. Sometimes it is possible to identify different processes by analyzing the shape of the

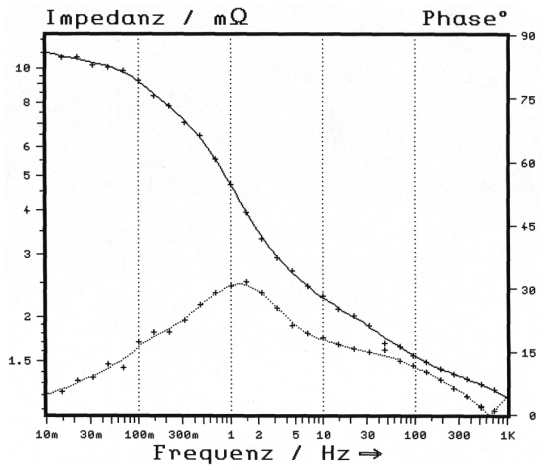

Fig.2: Cell impedance displayed as a Bode plot.

phase-angle. A turning point or a local minimum in the course of the phase angle indicates the border between two different processes. At the frequency of this minimum sometimes the recorded impedance may change the slope (Figure 2). Until now inside a MCFC quite a number of independent processes have been identified to contribute more or less to the recorded impedance data:

1) Contribution to ohmic Resistance
   - conductivity of the electrolyte
   - matrix thickness
   - conductivity of the metallic components
   - conductivity of the corrosion layers
   - conductivity of the cathode material
   - conductivity of the anode material

1) Contribution to the Polarization Resistance
   - Charge Transfer Process on cathode and anode
   - Diffusion of the reactants in the gas phase on anode or cathode side
   - Diffusion of the reactants in the liquid phase on anode or cathode side
   - Adsorption of the reactants on the anode or the cathode
   - Desorption of the products on the anode and cathode side
   - Nernst-Effects on anode and cathode side
   - .....

Each process has its characteristic impedance at a typical frequency. Some of them are of minor influence on the resulting impedance data. Typically the impedance spectra of MCFC single cells are dominated by the sum of the ohmic contributions (electrolyte, matrix thickness, and the conductivity of cathode and corrosion layers), the charge transfer on the cathode side, diffusion of the reactants on the cathode side (both liquid and gas phase) and the Nernst-contribution on the anode side.

This can easily be demonstrated by changing the concentration of the reactants in the feed gases or their utilization in the electrode reactions. For example increasing the O_2 and CO_2-concentration or decreasing their utilizations on the cathode side the contribution related to the diffusion processes be

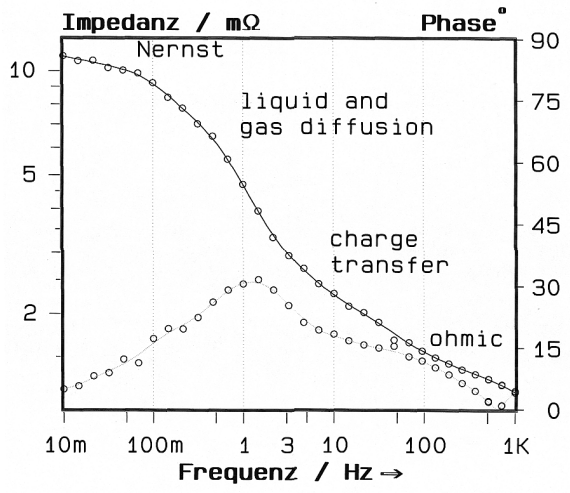

Fig.3: Bode plot of a cell measurement.

comes significantly smaller (Figure 4 - Impedance vs. Utilization [%]).

On the other hand the signal for the Nernst-Contribution can be identified by changing the utilization inside the anode gas (Figure 5 - Impedance vs. Utilization [%]).

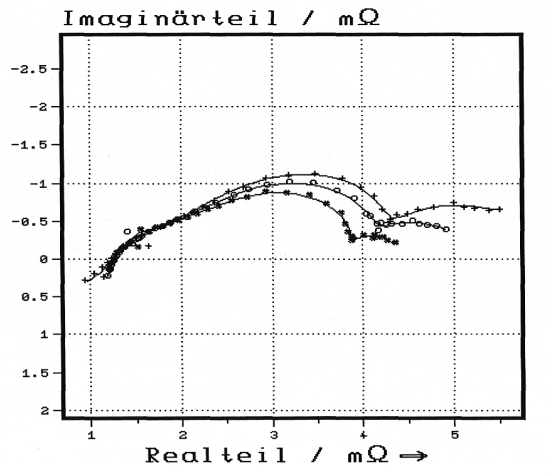

Fig.4: Influence of cathode gas utilization [%] on cathode impedance.

In general the shape of the impedance spectra depend strongly on the filling level of the porous components. In case of high filling level the gas phase diffusion has a low value but the liquid phase diffusion becomes remarkably high. Also the number of reaction sites on the surface of the electrodes may grow with increasing filling level. Therefore the charge transfer resistance may also be reduced at higher filling levels. On the other hand at low filling levels the ohmic contribution of the electrolyte and the liquid phase diffusion resistance becomes somewhat smaller while the contribution of the gas diffusion inside the pores may rise. Sometimes it is rather tricky to determine the optimum conditions for the measurements and of course for the operation.

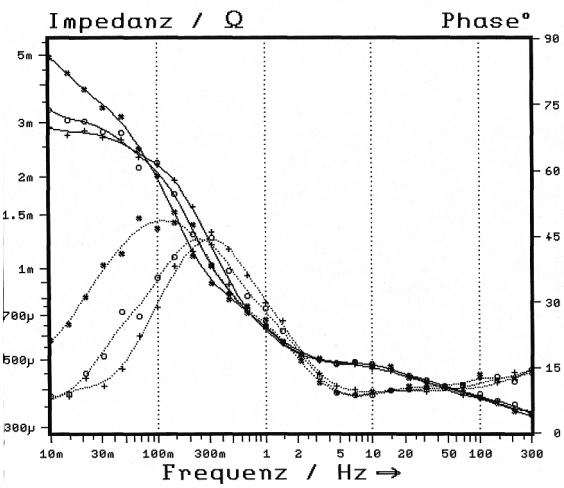

Fig.5: Influence of anode gas utilization [%] on anode impedance.

Rather interesting is the dependency of the impedance on the temperature. If the temperature is decreased from the operation temperature of 650°C down to 575°C the readings of the impedance will increase.

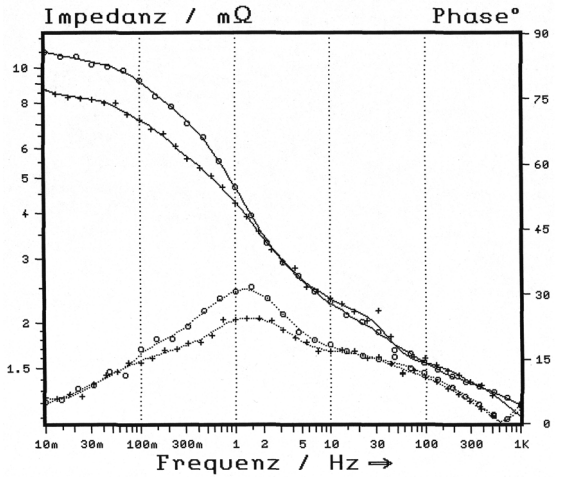

Fig.6: Influence of the filling level on cell impedance.

At certain temperatures different processes will dominate the overall reactivity – between 650 and 600 the diffusion process will be the rate limiting process while at lower temperatures the contribution of the charge transfer becomes more dominant (Figure 7 - Temperature given in [°C]).

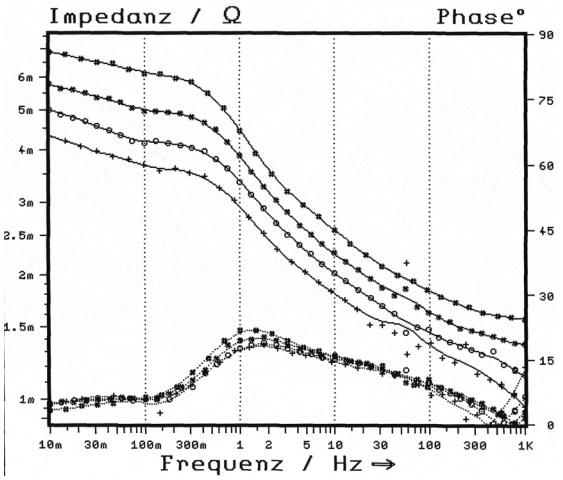

Fig. 7 Influence of the temperature [°C] on the cathode impedance

This can easily be determined applying the Arrhenius-Plot method (R vs. 1/T), where the resulting activation energies are displaying the dominant process (650 – 600°C – diffusion domination Ea ~ 30 - 50 kJ/mol; < 600°C – charge transfer dominated Ea ~ > 60 kJ/mol).

Conclusion

AC-impedance spectroscopy on MCFC allows identifying

- several individual reactions
- the influence of the modifications of single components, gas composition and temperature on the ohmic or on the polarization resistance.

Editorial
Electrochemical Applications is published by
Zahner-elektrik GmbH & Co. KG
Thüringer Str. 12, D-96317 Kronach, Germany
Tel.: 09261-52005 / Fax: 09261-51919
email: hjs@zahner.de
web: www.zahner.de

Editor:
Dr. Hans-Joachim Schäfer (Zahner-elektrik, Kronach)
Authors of this issue:
Dr. Joachim Hoffmann (MTU-Friedrichshafen, München), Dr. Franz Richter (Siemens AG, Erlangen), Carl-Albrecht Schiller (Zahner-elektrik, Kronach), Dr. Werner Strunz (Zahner-elektrik, Kronach), Dr. Norbert Wagner (DLR, Stuttgart)